Entanglement and disentanglement in circuit QED architectures

David Zueco [a], Georg M. Reuther [a], Peter Hänggi [a], Sigmund Kohler [a,b,*]

[a] Institut für Physik, Universität Augsburg, Universitätsstraße 1, D-86135 Augsburg, Germany
[b] Instituto de Ciencia de Materiales de Madrid, CISC, C/Sor Juana Inés de la Cruz 3, E-28049 Madrid, Spain

1. Introduction

The coupling between an atom and the quantized electromagnetic field represents a paradigmatic setup in quantum optics that allows one to study the interaction of light and matter in a fully quantum mechanical way. In most related experiments, an atom is placed inside a cavity, from where stems the labelling "cavity quantum electrodynamics" [1].

In the last years the implementation of such systems in the solid state realm has been demonstrated [2,3]. Depending on the experimental implementation, the atom is realized artificially with a superconducting circuit or a quantum dot, while a quantum LC-circuit as part of a transmission line or a photonic crystal, respectively, serves as cavity. This not only provides a widely enhanced tunability of parameters in an experiment, but also allows one to achieve the strong coupling limit between the artificial atom and the cavity, where the interaction exceeds the decay rates of the atom and the cavity by far. It has recently been shown that the coupling strength may even be enhanced by several orders of magnitude compared to conventional cavity QED experiments [4]. Furthermore, circuit QED systems may be used for many experimental validations of quantum mechanics, such as the quantum-non-demolition-like readout of a qubit state [5], the generation of Fock states [6], the observation of Berry phases [7], or multiphoton resonances [8]. Generation of entanglement between the qubit and the cavity via a Landau–Zener sweep has been theoretically proposed as well [9,10]. From a fundamental point of view these setups, realizing "quantum optics on a chip", give the opportunity to rediscover and improve the vast goals of quantum optics and to test experimentally its concepts in the solid state.

However, the mentioned experiments involve "only" a single qubit and one cavity. With a view to quantum computing, i.e. in order to realize a quantum register, it is highly desirable to couple several of these qubit–cavity systems to obtain a circuit QED network. This would not only allow for performing quantum operations such as quantum gates, but also enable the creation and distribution of entanglement throughout the network. Indeed, a setup to couple two cavities via an ancilla qubit has been recently proposed in Refs. [11,12], while in recent experiments [13,14], two qubits have been entangled via one cavity.

In this paper, referring to the setup of Ref. [11] we suggest the transfer of entanglement between two qubit–cavity systems via an ancilla qubit, which requires entangling different cavities. We restrict ourselves to the case where the qubit–cavity entanglement is created via a Landau–Zener sweep; cf. Refs. [9,10].

Due to the interaction with a dissipative environment, entanglement within an open quantum system is typically subject to decay via spontaneous emission. For the non-trivial class of states discussed here, this can even occur during finite time [15,16]. This phenomenon of "sudden death of entanglement" has been investigated theoretically for a conventional cavity QED setup [17] and observed in an experiment as well [18].

The paper is organized as follows. In Section 2 we shortly review the elementary description of a superconducting qubit coupled to an electromagnetic quantum circuit. Further, we give a brief review on the creation of entanglement between qubit and cavity by a Landau–Zener sweep. In Section 3 we discuss the influence of a dissipative environment on the final entangled qubit–cavity state. In Section 4 we consider a network architec-

* Corresponding author at: Institut für Physik, Universität Augsburg, Universitätsstraße 1, D-86135 Augsburg, Germany.
E-mail addresses: david.zueco@physik.uni-augsburg.de (D. Zueco), sigmund.kohler@icmm.csic.es (S. Kohler).

ture consisting of two qubit–cavity systems dynamically coupled via an ancilla qubit, and discuss how this dynamical interaction yields an entangled two-cavity state. Finally, in Section 5, we investigate the finite-time disentanglement of that state under environmental influence, depending on the details of state preparation.

2. Qubit–cavity entanglement via LZ sweep

Among many possible setups for circuit QED, one concrete realization is given by a Cooper pair box (CPB) that couples capacitively to a LC circuit, which acts as a harmonic oscillator [4]. The CPB is formed of a superconducting island connected to a superconducting reservoir by a dc SQUID. The effective Josephson energy $E_J = E_J^0 \cos(\pi\Phi/\Phi_0)$ can be tuned via an external flux Φ penetrating the SQUID, where Φ_0 denotes the flux quantum. We assume that Φ is switchable within a sufficiently large time interval such that $E_J = \hbar v t$, $v > 0$. The capacitive energy of the CPB, $E_{el} = \frac{1}{2}E_c(N - N_g)^2$ is determined by the geometry-dependent charging energy E_c, the number N of Cooper pairs on the island, and the reduced background charge N_g which is proportional to a voltage bias V_g. In the charging limit $E_c \gg E_J$ and near the charge degeneracy point $N_g = \frac{1}{2}$, it is justified to describe the CPB by its two lowest charge states $|N = 0\rangle$ and $|N = 1\rangle$. This allows the interpretation as a two-level system (TLS) or qubit for which the Hamiltonian in pseudo-spin notation reads $H_{qb} = -\frac{1}{2}\hbar v t \sigma_z$. It possesses the eigenstates $|\uparrow\rangle = (|0\rangle + |1\rangle)/\sqrt{2}$ and $|\downarrow\rangle = (|0\rangle - |1\rangle)/\sqrt{2}$.

Making use of the standard Rabi model the total qubit–oscillator Hamiltonian reads [4]

$$\mathscr{H}_s = -\frac{\hbar v t}{2}\sigma_z + \hbar g \sigma_x (a^\dagger + a) + \hbar \Omega a^\dagger a. \tag{1}$$

The second term refers to the coupling of the qubit to the fundamental mode of the transmission line, which is modelled as a harmonic oscillator with the usual bosonic creation and annihilation operators $a^\dagger$ and a and energy eigenstates $|n\rangle$, $n = 0, 1, \ldots, \infty$. Note that the usually performed rotating wave approximation (RWA) in the coupling Hamiltonian is not justified here since during almost the complete Landau–Zener sweep, the qubit and the harmonic oscillator are far detuned.

If the effective Josephson energy is switched from a large negative to a large positive value, and assuming that both the TLS and the oscillator are initially in their ground state $|\uparrow, 0\rangle$, the probability for the TLS to end up in the upper state can be computed exactly to read [10]

$$P_{\uparrow\to\downarrow} = 1 - e^{-2\pi g^2/v}. \tag{2}$$

This clearly reminds one of the Landau–Zener formula for the bare two-level system [19–21], with the level splitting in the anticrossing at $t = \Omega/v$ (see Fig. 1) now given by the coupling constant g. It should be noted that the probability (2) does not provide any direct information about the final oscillator state. However, due to the symmetry of the Hamiltonian (1), every creation or annihilation of a photon is accompanied by a qubit flip, which restricts the resulting dynamics to the states $|\uparrow, 2n\rangle$ and $|\downarrow, 2n+1\rangle$. Furthermore, the "no-go-up" theorem states that $P_{\uparrow,n\to\uparrow,m} = 0$ for $m > n$ [22]. This reduces the possible final qubit–oscillator states to the state

$$|\psi(\infty)\rangle = \sqrt{1 - P_{\uparrow\to\downarrow}}\,|\uparrow, 0\rangle + \sqrt{P_{\uparrow\to\downarrow}}\sum_n c_n |\downarrow, 2n+1\rangle \tag{3}$$

with the normalization $\sum_n |c_n|^2 = 1$. In the experimentally relevant limit of $g \ll \Omega$, we numerically find that during

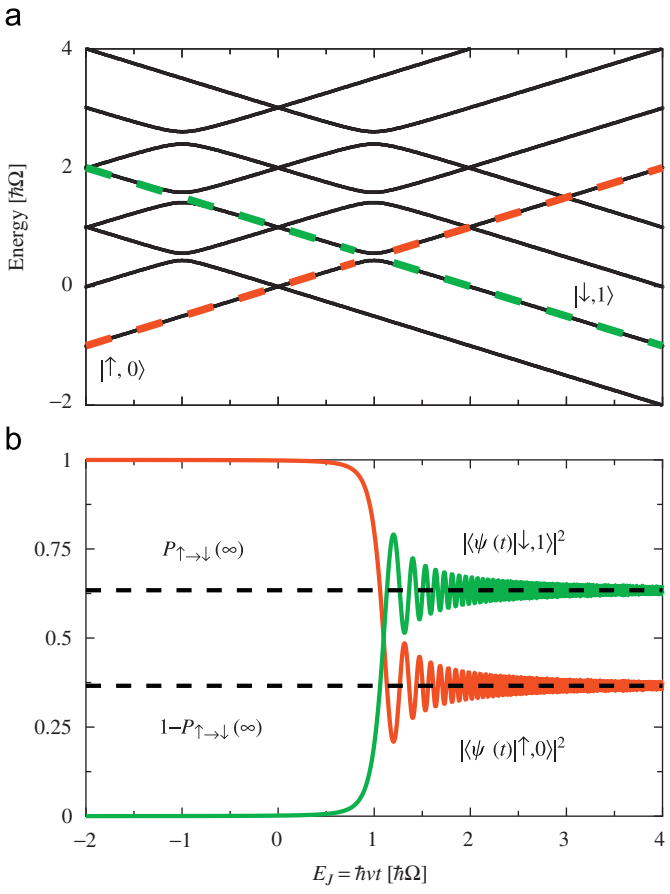

Fig. 1. (Color online) (a) Adiabatic energy levels of the qubit–oscillator Hamiltonian (1) as a function of the Josephson energy which is swept at constant velocity such that $E_J = \hbar v t$. Here, $g = 0.04\Omega$ and $v = 0.01\Omega^2$. (b) Dynamics for the probabilities $|\langle\downarrow, 1|\psi(t)\rangle|^2$ and $|\langle\uparrow, 0|\psi(t)\rangle|^2$. The occupation of higher states is always less than 0.01% (not shown).

the whole Landau–Zener transition, the state is well approximated by

$$|\psi(t)\rangle \cong \alpha(t)|\uparrow, 0\rangle + \beta(t)|\downarrow, 1\rangle \tag{4}$$

with $\alpha(\infty) = \sqrt{1 - P_{\uparrow\to\downarrow}}$, and $\beta(\infty) = \sqrt{P_{\uparrow\to\downarrow}}c_1$, i.e. $|c_1| \cong 1$. We substantiate this by plotting a typical example for the characteristics of the LZ dynamics in Fig. 1(b), where it becomes evident that finally only the states $|\uparrow, 0\rangle$ and $|\downarrow, 1\rangle$ are significantly populated. This means a great simplification since it allows one to reduce the number of all relevant oscillator states to two.

Then in particular, the qubit–oscillator state (4) is entangled and can therefore be mapped to the state of two entangled two-level systems. For future convenience it is useful to introduce the density matrix for the qubit–cavity system $\rho_{q-c} = |\psi\rangle\langle\psi|$ that reads, in the basis $\{|\uparrow, 0\rangle, |\downarrow, 0\rangle, |\uparrow, 1\rangle, |\downarrow, 1\rangle\}$,

$$\rho_{q-c}(t) = \begin{pmatrix} |\alpha(t)|^2 & 0 & 0 & \alpha^*(t)\beta(t) \\ 0 & 0 & 0 & 0 \\ 0 & 0 & 0 & 0 \\ \alpha(t)\beta^*(t) & 0 & 0 & |\beta(t)|^2 \end{pmatrix}. \tag{5}$$

As a consequence, we can use the concurrence as a well-defined measure of entanglement for the two two-level systems. It is defined as $C = \max\{\lambda_1 - \lambda_2 - \lambda_3 - \lambda_4, 0\}$. The parameters λ are the ordered eigenvalues of the matrix $\sqrt{\rho}(\sigma_y^c \otimes \sigma_y^q)\rho(\sigma_y^c \otimes \sigma_y^q)\sqrt{\rho}$ [23]. Here, the Pauli matrices σ_y^q and σ_y^c act on the qubit space and the reduced

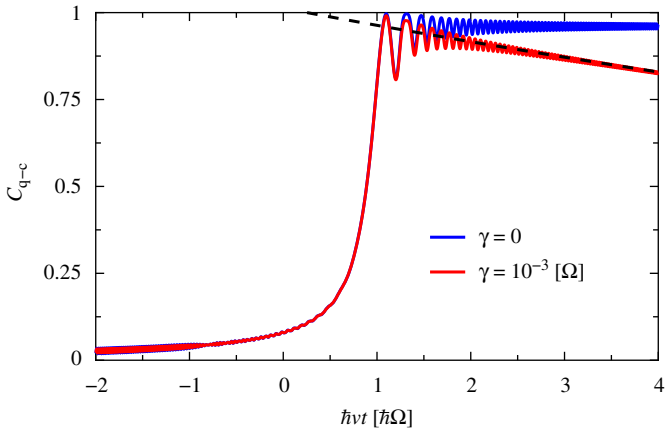

Fig. 2. Qubit–oscillator entanglement in terms of the concurrence C_{q-c} for a Landau–Zener transition. Here, $k_BT = 0.01\hbar\Omega$, while g and v are as in Fig. 1. For finite coupling strength $\gamma > 0$ (red line), the decay of the concurrence is approximated by expression (11) (dashed black line). For comparison, the concurrence is also given for the case of vanishing interaction with the environment (blue line). (For interpretation of the references to color in this figure legend, the reader is referred to the web version of this article.)

oscillator space formed by the states $|0\rangle$ and $|1\rangle$, respectively. For the density matrix (5), the concurrence is given by

$$C_{q-c} = 2|\alpha^*(t)\beta(t)|. \tag{6}$$

Thus, the amount of entanglement in the long-time limit is given by $C_{q-c}(\infty) = 2\sqrt{(1-P_{\uparrow\to\downarrow})P_{\uparrow\to\downarrow}}$, which just depends on the ratio g^2/v. As an example, we plot the typical dynamics for the concurrence in Fig. 2, from where it is evident that entanglement is created after passing the anticrossing.

3. Influence of the dissipative environment

In a realistic experimental scenario, the qubit–oscillator system has to be regarded as an open system, i.e. one that interacts with its environment, thus suffering dissipation and decoherence. Dissipative effects in an electromagnetic circuit are characterized by a spectral density $I(\omega)$ which, within a quantum mechanical description, can be modelled by coupling the circuit bi-linearly to the field modes of an electromagnetic environment [24]. For weak system–bath coupling, tracing out the bath degrees of freedom and following standard techniques, the bath can be eliminated within Bloch–Redfield theory [25,26] yielding the quantum master equation

$$\begin{aligned}\dot\rho &= -\frac{i}{\hbar}[\mathscr{H}_s,\rho] - \frac{1}{\hbar}[Q,[\hat Q,\rho]] - i\frac{Z_0}{\hbar}[Q,[\dot Q,\rho]_+] \\ &\equiv -\frac{i}{\hbar}[\mathscr{H}_s,\rho] + \mathscr{L}\rho,\end{aligned} \tag{7}$$

with the anticommutator $[A,B]_+ = AB + BA$, the oscillator-bath coupling operator $Q = a^\dagger + a$ and the operators $\dot Q = i[\mathscr{H}_s, Q]/\hbar$ and

$$\hat Q = \frac{1}{\pi}\int_0^\infty d\tau \int_0^\infty d\omega\, S(\omega)\cos(\omega\tau)\tilde Q(-\tau). \tag{8}$$

Here, $S(\omega) = I(\omega)\coth(\hbar\omega/2k_BT)$ is the Fourier transform of the symmetrically ordered equilibrium correlation function for a thermal environment at temperature T. We assume the spectral density to be ohmic, i.e. $I(\omega) = \omega\gamma$ with an effective impedance γ. The notation $\tilde X(t)$ is a shorthand for the Heisenberg operator $U_0^\dagger(t)XU_0(t)$, where U_0 is the system propagator. While the quantum master equation (7) is general, an explicit form with respect to the Hamiltonian (1), together with details about the numerical implementation can be found in Ref. [27].

3.1. Entanglement creation

Due to the influence of the environment, in particular, the entanglement created between qubit and cavity is subject to decay during the Landau–Zener sweep. In the case of low temperatures, $k_BT \sim 0.01\hbar\Omega$, which is relevant for most experiments, our numerical investigations of the master equation (7) confirm the following scenario: Before reaching the first avoided crossing at time $t < -\Omega/v$ (see Fig. 1), the system remains in its ground state. Then at time $t = -\Omega/v$, it evolves into the superposition (4). Simultaneously, the bath causes coherence decay and, for low temperature, a relaxation from the state $|\uparrow,1\rangle$ to $|\uparrow,0\rangle$ occurs. We emphasize here that there is no transition $|\uparrow,0\rangle \to |\downarrow,0\rangle$ since the qubit experiences an effective heat bath with a spectral density sharply peaked at the oscillator frequency Ω [28–31]. Thus, for large times $t \gg \Omega/v$, the spectral density at the qubit splitting $\hbar vt$ vanishes and, consequently, the qubit is effectively decoupled from the bath. As a consequence, we numerically find that after the anticrossing the state $|\downarrow,0\rangle$ becomes populated in addition to the states $|\uparrow,0\rangle$ and $|\downarrow,1\rangle$. Quantitatively, the corresponding density matrix takes the form [cf. (5)]

$$\rho_{q-c}(t) = \begin{pmatrix} a & 0 & 0 & c \\ 0 & z & 0 & 0 \\ 0 & 0 & 0 & 0 \\ c^* & 0 & 0 & d \end{pmatrix}. \tag{9}$$

After the Landau–Zener transition, its entries can be well approximated by

$$\begin{aligned} a &= 1 - P_{\uparrow\to\downarrow}, \\ d &\cong P_{\uparrow\to\downarrow}\mathrm{e}^{-\gamma(t-\tau_{LZ})}, \\ z &\cong P_{\uparrow\to\downarrow}(1-\mathrm{e}^{-\gamma(t-\tau_{LZ})}), \\ |c| &\cong \sqrt{P_{\uparrow\to\downarrow}(1-P_{\uparrow\to\downarrow})}\mathrm{e}^{-\gamma(t-\tau_{LZ})}, \end{aligned} \tag{10}$$

where $\tau_{LZ} = \Omega/v$ and $P_{\uparrow\to\downarrow}$ has been defined in Eq. (2). For the state (9), the concurrence is now given by

$$C_{q-c} = 2|c| \cong 2\sqrt{P_{\uparrow\to\downarrow}(1-P_{\uparrow\to\downarrow})}\mathrm{e}^{-\gamma(t-\tau_{LZ})}. \tag{11}$$

Hence the loss of entanglement is directly related to the loss of coherence between the qubit and the cavity and exhibits a simple exponential decay, see Fig. 2.

4. Qubit–cavity networks

In this section we discuss how entanglement may be created within a quantum network architecture consisting of several pairs of cavities and qubits. We shall make use of the setup proposed in Ref. [12] together with the state preparation via a Landau–Zener sweep discussed above, in order to entangle two cavities. We study the resulting dynamics in presence of dissipation and decoherence. The setup we have in mind is sketched in Fig. 3, and consists of two qubit–cavity systems. The cross geometry indicates that qubit A (B) is only coupled to cavity A (B) whereas the central qubit (ancilla) is coupled to both cavities and may be used as a switch, as we will explain below. The Hamiltonian of such a system can be

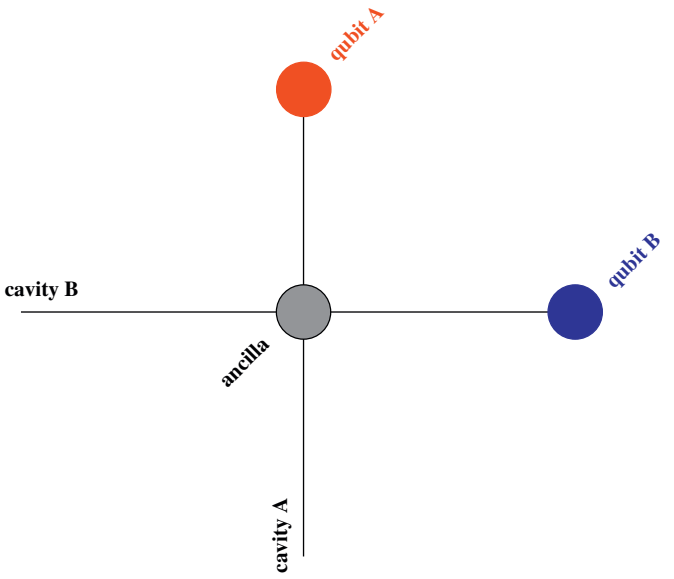

Fig. 3. (Color online) Sketch of the quantum network under consideration. Qubits are represented by big dots and cavities by black lines. Qubit A (B) is only coupled to cavity A (B), whereas both cavities may effectively interact with each other by the ancilla qubit.

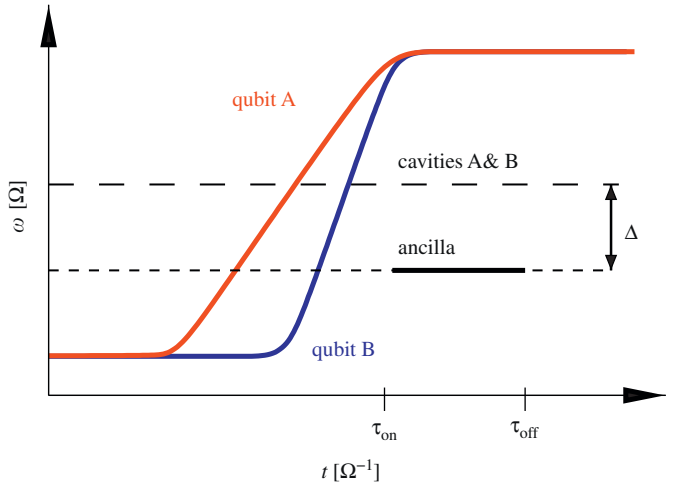

Fig. 4. (Color online) Sketch of the quantum switch protocol, displaying the time-dependent qubit and cavity energies and the ancilla interaction: The qubits A and B undergo Landau–Zener sweeps with their respective cavities with velocities v_A and v_B. This leads to the entangled qubit–cavity state (4). Meanwhile, the cavities do not interact, i.e. $g_{SW}=0$ (dashed line). From $t=\tau_{on}$ to $t=\tau_{off}$, $g_{SW}>0$ (solid line), leading to the entangled state (15) which is subject to decay for $t>\tau_{off}$. For further details, see text.

approximated as

$$H=-\sum_{\mu=A,B}\left\{\frac{E_J^{\mu}(t)}{2}\sigma_z^{\mu}-\hbar g(a_{\mu}^{\dagger}+a_{\mu})\sigma_x^{\mu}+\Omega a_{\mu}^{\dagger}a_{\mu}\right\}$$
$$+\frac{\omega_{anc}(t)}{2}\sigma_z^{anc}+(g_x\sigma_x^{anc}+g_z\sigma_z^{anc})\sum_{i=1,2}(a_j^{\dagger}+a_j)$$
$$+G(a_A^{\dagger}+a_A)(a_B^{\dagger}+a_B). \qquad (12)$$

The first line of Eq. (12) denotes the usual Rabi Hamiltonians for the, respectively, coupled qubits and cavities. For simplicity, both cavities are supposed to have the same frequency Ω. The second line describes the ancilla qubit and its coupling to the cavities, whereas the last line accounts for the direct geometrical interaction between the cavities which will be referred to as "geometrical coupling" [11] (see Fig. 4).

4.1. The entanglement protocol

In order to entangle the cavities A and B, we pursue a "quantum switching protocol" in analogy to the procedure described in Ref. [11]: In order to reach the dispersive coupling regime $g_x/\Delta\ll 1$ between ancilla and cavities with the detuning $\Delta=\omega_{anc}-\Omega$, the ancilla qubit is widely detuned from the cavity frequency [4]. On the other hand, $\Delta\ll\Omega$, which allows a rotating-wave approximation with respect to the ancilla–oscillator coupling. Under this condition the ancilla gives rise to an effective "dynamical coupling" between the cavities which may be expressed as $g_x^2\sigma_z(a_A^{\dagger}a_B+a_Aa_B^{\dagger})/\Delta$. The total interaction between both cavities including the additional geometrical coupling [last line of Eq. (12)] is then given by

$$H_{int}=g_{SW}(a_A^{\dagger}a_B+a_Aa_B^{\dagger}),\quad g_{SW}=\frac{g_x^2}{\Delta}\sigma_z+G. \qquad (13)$$

It is possible to "switch off" this interaction by setting g_{SW} to zero. This requirement can be fulfilled varying Δ or g_x, or manipulating the state of the ancilla. The protocol is now performed as follows: At first stage, both cavities and qubits become entangled via Landau–Zener sweeps at different sweep velocities v_A and v_B, while the ancilla is in the "off" state, $g_{SW}=0$. After the Landau–Zener sweeps, the state of the total system is the product state

$$\rho_{cav,i}(t)=\rho_{qA-cA}\otimes\rho_{qB-cB}, \qquad (14)$$

where $\rho_{q,A/B-cq,A/B}$ are of the form (9). At this point, there is no entanglement between any object of A and B. Once the state (14) is achieved, the interaction is "turned on" towards a finite interaction strength $g_{SW}>0$ at time $t=\tau_{on}$. This may be accomplished e.g. by changing adiabatically the operational point of the ancilla, which modifies Δ [11]. In the following, correlations between the cavities A and B emerge by virtue of the interaction (13). At time $t=\tau_{off}$, the interaction is turned off again. As far as we are only interested in the entanglement dynamics of the cavities, we may trace out the qubit and ancilla degrees of freedom in Eq. (14). For $\tau_{off}-\tau_{on}=\pi/4g_{SW}$ the resulting density matrix $\rho_{cav,f}$ takes the form

$$\rho_{cav,f}=\begin{pmatrix}\overline{\alpha} & 0 & 0 & 0\\ 0 & \frac{1}{2}(z_1+z_2) & \frac{-i}{2}(z_1-z_2) & 0\\ 0 & \frac{i}{2}(z_1-z_2) & \frac{1}{2}(z_1+z_2) & 0\\ 0 & 0 & 0 & \overline{\beta}\end{pmatrix} \qquad (15)$$

in the basis $\{|0_A0_B\rangle,|0_A1_B\rangle,|1_A0_B\rangle,|1_A1_B\rangle\}$. For simplicity, we have introduced the notations

$$\overline{\alpha}=a_Aa_B+a_Az_B+a_Bz_A+z_Az_B,$$
$$\overline{\beta}=d_Ad_B,$$
$$z_1=(z_A+a_A)d_B,$$
$$z_2=(z_B+a_B)d_A. \qquad (16)$$

The coefficients $a_{A/B}$, $d_{A/B}$ and $z_{A/B}$ are defined in Eq. (10), where the indices A and B refer to the respective cavities. This reveals the dependence of the final state $\rho_{cav,f}$ on the specific parameters of our particular entanglement protocol. We point out that the most relevant parameters for the preparation of Eq. (15) are the Landau–Zener sweep velocities v_A and v_B. The corresponding concurrence is given by

$$C_{cav,f}=2\max\left\{0,\tfrac{1}{2}|z_1-z_2|-\sqrt{\overline{\alpha}\overline{\beta}}\right\}. \qquad (17)$$

As a result, using the state preparation via Landau–Zener sweeps together with the quantum switching protocol described above, we end up with both cavities being in an entangled state that depends on the particular parameters of the protocol. The individual entanglement between the individual qubit–oscillator systems has thus been *transferred* via cavity–cavity entanglement.

5. Finite-time disentanglement

In the presence of a dissipative environment of each cavity, the entanglement between the two cavities is naturally subject to decay. Now the possibility of finite-time disentanglement in a quantum optical setup due to spontaneous emission has been reported in Refs. [17,32] for the special class of entangled two-cavity states such as $\rho_{\mathrm{cav,f}}$; see Eq. (15). In this case the concurrence $C(t)$ decays within a finite time, depending on the initial state and thus on the particular state preparation. This signifies a "sudden death of (non-local) entanglement" whereas the decay characteristics of local decoherence is exponential. Finite-time disentanglement has also been observed in a recent experiment [18].

In the following, we study the disentanglement of the state $\rho_{\mathrm{cav,f}}$. Again, as an important point, our proposed circuit QED setup and protocol would allow for this to be analyzed in the solid state realm, while Refs. [17,32] refer to an optical cavity QED setup.

We start with the effective Hamiltonian for the uncoupled cavities

$$\mathscr{H}^{\mathrm{eff}}_{\mathrm{cav,f}} = \hbar\Omega(a_A^\dagger a_A + a_B^\dagger a_B). \tag{18}$$

Following Section 2, we may restrict the description of the cavities to the two lowest Fock states. In order to investigate the time evolution of the entangled two-cavity state $\rho_{\mathrm{cav,f}}$ after the ancilla interaction has been set to zero at $t = \tau_{\mathrm{off}}$, we solve the quantum master equation

$$\dot{\rho} = -\frac{i}{\hbar}[\mathscr{H}^{\mathrm{eff}}_{\mathrm{cav,f}}, \rho] + \mathscr{L}_A[a_A + a_A^\dagger]\rho + \mathscr{L}_B[a_B + a_B^\dagger]\rho, \tag{19}$$

where the Liouvillian $\mathscr{L}_{A/B}$ is defined as in Eq. (7). Hence we assume both entangled cavities to interact individually with vacuum noise, i.e. to interact with individual environments. A scenario with two two-level systems with zero distance, i.e. coupled to the same environment, was discussed in Ref. [33].

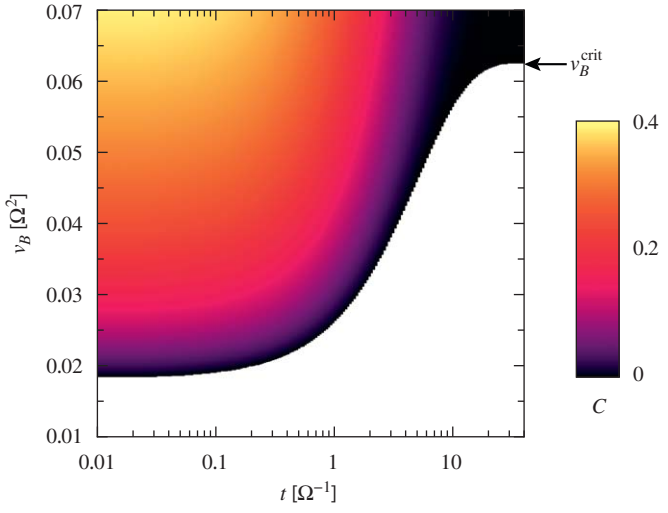

Fig. 5. (Color online) Time evolution of the concurrence $C_{\mathrm{cav}}(t)$ starting with state $\rho_{\mathrm{cav,v}}$. Here, $v_A = 0.005\Omega^2, g_A = g_B = 0.04\Omega$ and $T = 0.001\Omega$. White color corresponds to separable states. Here, $v_B^{\mathrm{crit}} = 0.0624\Omega^2$.

In Fig. 5 we plot the concurrence $C_{\mathrm{cav}}(t)$ for the decaying state $\rho_{\mathrm{cav,f}}$ as a function of time and the sweep velocity v_B, while keeping v_A constant. We find that the concurrence drops to zero at a finite time $t \geq t_{\mathrm{d}}$ for a broad range of different values of v_B. This indicates that the corresponding initial states become disentangled after a finite time. However, this does not always hold: For $v_B > v_B^{\mathrm{crit}}$ we rather find exponential concurrence decay, i.e. $t_{\mathrm{d}} = \infty$. Note that, in contrast to these results, the qubit–cavity entanglement always decays exponentially as discussed in Section 3.

Our results comply perfectly with the disentangling behavior discussed by Yu and Eberly [17], which underlines the generic nature of that scenario.

6. Conclusions

We have proposed a protocol for creating an entangled two-cavity state within a circuit QED network architecture. Thereby, we have considered a network of two superconducting qubits each coupled to an electromagnetic quantum circuit. While there is no direct interaction between the qubits, the cavities are connected through a third "ancilla" qubit. Depending on its state and its detuning from the cavities, this coupling may be switched on and off. As first protocol step, one has to prepare two entangled qubit–cavity states, which we have suggested to be done via Landau–Zener sweeps. Note that there exist other possibilities for this purpose, for example by Rabi oscillations. Second, the interaction is "switched on" in order to entangle both cavities. At the same time we have considered the influence of a separate dissipative environment for each cavity.

A major goal here is the preparation of an entangled two-cavity state such as (15). In the quantum optics community this class of states has been proposed to investigate finite-time disentanglement due to spontaneous emission. Here we have shown that this can be done as well in the solid state realm, depending on the particulars of state preparation. The entries of the density matrix (15) can be obtained by measuring cross-correlations between the cavities. A corresponding circuit QED experiment has been proposed recently [34]. Thus, we belief that our protocol will enable experimentalists to study non-trivial dynamics of entanglement in quantum circuits.

Acknowledgments

We thank Frank Deppe and Matteo Mariantoni for fruitful discussions. This work has been supported by DFG through SFB 631 and by the German Excellence Initiative via "Nanosystems Initiative Munich (NIM)".

References

[1] H. Walther, B.T.H. Varcoe, B.-G. Englert, T. Becker, Rep. Progr. Phys. 69 (2006) 1325.
[2] A. Wallraff, D.I. Schuster, A. Blais, L. Frunzio, R.-S. Huang, J. Majer, S. Kumar, S.M. Girvin, R.J. Schoelkopf, Nature 431 (2004) 162.
[3] K. Hennessy, A. Badolato, M. Winger, D. Gerace, M. Atatüre, S. Gulde, S. Fält, E.L. Hu, A. Imamoglu, Nature 445 (2007) 896.
[4] A. Blais, R.-S. Huang, A. Wallraff, S.M. Girvin, R.J. Schoelkopf, Phys. Rev. A 69 (2004) 062320.
[5] A. Lupascu, S. Saito, T. Picot, P.C. de Groot, C.J.P.M. Harmans, J.E. Mooij, Nat. Phys. 3 (2007) 119.
[6] M. Hofheinz, E.M. Weig, M. Ansmann, R.C. Bialczak, E. Lucero, M. Neeley, A.D. O'Connell, H. Wang, J.M. Martinis, A.N. Cleland, Nature 454 (2007) 310.
[7] P.J. Leek, J.M. Fink, A. Blais, R. Bianchetti, M. Göppl, J.M. Gambetta, D.I. Schuster, L. Frunzio, R.J. Schoelkopf, A. Wallraff, Science 318 (2007) 1889.

[8] F. Deppe, M. Mariantoni, E.P. Menzel, A. Marx, S. Saito, K. Kakuyanagi, H. Tanaka, T. Meno, K. Semba, H. Takayanagi, E. Solano, R. Gross, Nat. Phys. 4 (2008) 686.
[9] M. Wubs, S. Kohler, P. Hänggi, Physica E 40 (2007) 187.
[10] K. Saito, M. Wubs, S. Kohler, P. Hänggi, Y. Kayanuma, Europhys. Lett. 76 (2006) 22.
[11] M. Mariantoni, F. Deppe, A. Marx, R. Gross, F.K. Wilhelm, E. Solano, Phys. Rev. B 78 (10) (2008) 104508.
[12] F. Helmer, M. Mariantoni, A.G. Fowler, J. von Delft, E. Solano, F. Marquardt, EPL 85 (2009) 50007.
[13] M.A. Sillanpää, J.I. Park, R.W. Simmonds, Nature 449 (2007) 438.
[14] J. Majer, J.M. Chow, J.M. Gambetta, J. Koch, B.R. Johnson, J.A. Schreier, L. Frunzio, D.I. Schuster, A.A. Houck, A. Wallraff, A. Blais, M.H. Devoret, S.M. Girvin, R.J. Schoelkopf, Nature 449 (2007) 443.
[15] K. Ann, G. Jaeger, Phys. Rev. A 76 (2007) 044101.
[16] K. Ann, G. Jaeger, Phys. Lett. A 372 (2008) 579.
[17] T. Yu, J.H. Eberly, Phys. Rev. B 66 (2002) 193306.
[18] M.P. Almeida, F. de Melo, M. Hor-Meryll, A. Salles, S.P. Walborn, P.H.S. Ribeiro, L. Davidovich, Science 316 (2007) 579.
[19] L.D. Landau, Phys. Z. Sowjetunion 2 (1932) 46.
[20] C. Zener, Proc. Roy. Soc. London Ser. A 137 (1932) 696.
[21] E.C.G. Stueckelberg, Helv. Phys. Acta 5 (1932) 369.
[22] K. Saito, M. Wubs, S. Kohler, Y. Kayanuma, P. Hänggi, Phys. Rev. B 75 (2007) 214308.
[23] W.K. Wootters, Phys. Rev. Lett. 80 (1998) 2245.
[24] B. Yurke, J.S. Denker, Phys. Rev. A 29 (1984) 1419.
[25] A.G. Redfield, IBM J. Res. Develop. 1 (1957) 19.
[26] K. Blum, Density Matrix Theory and Applications, Springer, New York, 1996.
[27] D. Zueco, P. Hänggi, S. Kohler, New J. Phys. 10 (11) (2008) 115012.
[28] M. Thorwart, L. Hartmann, I. Goychuk, P. Hänggi, J. Modern Opt. 47 (2000) 2905.
[29] M. Thorwart, E. Paladino, M. Grifoni, Chem. Phys. 296 (2004) 333.
[30] F.K. Wilhelm, S. Kleff, J. von Delft, Chem. Phys. 296 (2004) 345.
[31] F. Nesi, M. Grifoni, E. Paladino, New J. Phys. 9 (2007) 316.
[32] J.P. Paz, A.J. Roncaglia, arXiv:0809.167v1 quant-ph.
[33] R. Doll, M. Wubs, P. Hänggi, S. Kohler, Europhys. Lett. 76 (2006) 547.
[34] M. Mariantoni, M.J. Storcz, F.K. Wilhelm, W.D. Oliver, A. Emmert, A. Marx, R. Gross, H. Christ, E. Solano, cond-mat/0509737, 2005.